

## Thermoelectric power of single-walled carbon nanotube films

H. E. Romero, G. U. Sumanasekera, G. D. Mahan, and P. C. Eklund\*

*Department of Physics, Pennsylvania State University, University Park, Pennsylvania 16802*

(Received 1 November 2001; revised manuscript received 4 February 2002; published 13 May 2002)

We report measurements of the thermoelectric power (TEP)  $S$  and electrical resistance  $R$  of thin films of tangled ropes of single-walled carbon nanotubes. Experiments at 300 K under applied force normal to the plane of the film revealed a  $\sim 10$ – $20$  % decrease in the four-probe resistance, indicating that the contact resistance between ropes had improved. The TEP, however, was not affected by the applied force and the concomitant decrease in the contact resistance between ropes. A quasilinear, diffusion TEP is observed for temperatures  $T \geq 120$  K, indicating that the metallic tubes provide the dominant contribution. As the sample is heated in a vacuum (degassed), the TEP is observed to decrease with time and changes sign, retaining its metallic character. This behavior is explained as a consequence of the balance between charge  $O_2^{-\delta}$  species which can be removed by degassing and an unidentified donor state. In fact, by stopping the degassing process at the appropriate time, one can achieve a  $S \sim 0$  state over the range  $4 \text{ K} < T < 500 \text{ K}$ . Model calculations of the TEP are presented which show that the small TEP is identified with the near mirror symmetry bands in metallic tubes and that the Fermi energy of the rope is determined by the balance of acceptor and donor states on the semiconducting tubes. A broad low- $T$  feature in the TEP with maxima in the range  $80 \text{ K} < T < 100 \text{ K}$  is tentatively identified with phonon drag.

DOI: 10.1103/PhysRevB.65.205410

PACS number(s): 61.46.+w, 65.80.+n, 73.22.-f

### I. INTRODUCTION

In this paper, we present the results of a systematic study on a purified thin film of tangled single-walled nanotube (SWNT) ropes that show that the TEP is determined by coordinated effects in both the semiconducting and metallic tubes. However, the TEP will be shown to be dominated by the metallic tubes in the ropes. The sign and magnitude of the TEP will be shown to be determined by the relative concentration of  $O_2^{-\delta}$  (acceptor state;  $\delta$ =fractional charge) and an unidentified donor state on the semiconducting tubes, possibly due to wall defects. In fact, we show that a fully compensated sample can exhibit a thermopower  $S \sim 0$  over a wide temperature range ( $4 < T < 500$  K). In this case, we will argue that the Fermi energy for a rope containing semiconducting and metallic tubes is very near the intrinsic position. Furthermore, in this case, the mirror symmetry of the metallic band structure contributes offsetting contributions from electrons and holes.

The unique electrical properties of carbon nanotubes continue to attract considerable interest because of their extraordinary nature and potential applications.<sup>1</sup> Thermoelectric power, in particular, is sensitive to the balance of electrons and holes and their mobilities in a material, and therefore should be a valuable tool to elucidate the intrinsic electrical transport properties of SWNT's.<sup>2-4</sup> The temperature dependence of the TEP of mats or thin films containing bundles of single-walled carbon nanotubes has been shown to exhibit a dominant quasilinear component that can be surprisingly large  $S \sim +40 \mu\text{V/K}$  at 300 K, depending on the sample history.<sup>4</sup> This quasilinear behavior suggests that metallic tubes in the film dominate the TEP. This behavior is consistent with diffusive, not ballistic transport. A second, smaller, contribution to  $S$ , in the form of a superimposed broad peak with a maximum in the range  $\sim 100$ – $150$  K, can also be present.<sup>4</sup> This broad peak has been attributed to the Kondo

effect involving residual magnetic catalyst (e.g., Fe, Ni, Co) residing as particles on the bundles or rope surface, or trapped as atoms or small clusters within the bundles.<sup>4,5</sup> Further support for this assignment is that the chemical treatment to remove the metal, i.e., acid purification or treatment with iodine,<sup>4</sup> significantly reduces the Kondo contribution.

Recent studies<sup>6,7</sup> have found that the measured SWNT electronic properties are extremely sensitive to the presence of molecular oxygen. By TEP and resistivity measurements, they have shown that SWNT's can be easily doped by ambient exposure to  $O_2$  forming a charge transfer complex  $C_p^{+\delta}-O_2^{-\delta}$ . For the semiconducting tubes, the position of the Fermi level must shift toward the valence band. Furthermore, the TEP of the ropes is observed to change sign. These results demonstrated that the previously published large positive TEP data should not be considered as the intrinsic SWNT behavior, but rather the result of oxygen doping. In contrast to this view, Derycke *et al.*<sup>8</sup> have demonstrated a similar behavior using SWNT field effect transistors (CNT FET), i.e., the  $p$ -type electronic character can be turned into a fully  $n$ -type one by simply annealing in vacuum. Based on the observation that oxygen treatment has no effect on the threshold voltage for turning on a CNT FET, they argue that contact barriers control the carrier injection even though doping may take place. According to Derycke *et al.*, the dependence of these barriers on oxygen determines the electrical character of the CNT FET's.

### II. EXPERIMENTAL DETAILS

The SWNT's studied in our experiments were in the form of a thin film of tangled ropes deposited from an ethanol solution onto a quartz substrate. The SWNT material was obtained from Carboxlex, Inc. and consisted of  $\sim 50$ – $70$  vol % carbon as SWNT's produced by the arc discharge method using a Ni-Y catalyst. Purification of this

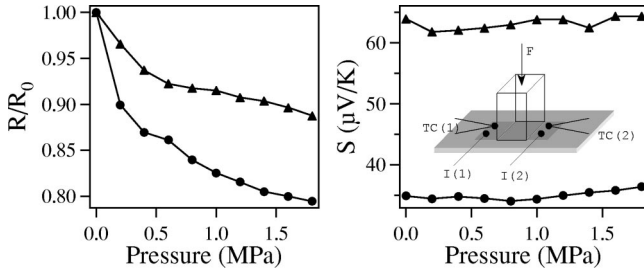


FIG. 1. Uniaxial pressure dependence of the normalized room temperature resistance ( $R/R_0$ ) and thermopower  $S$  for two different SWNT mats. The inset shows the experimental geometry where the applied force  $F$  is perpendicular to the sample.

material was done first by a selective oxidation step at 425 °C in dry air for  $\sim 20$  min to remove amorphous carbon and weaken the carbon shell covering the metal catalyst. This treatment was followed by a 28 hr. acid reflux in 4.0 M HCl to remove the metal residue. The material was then vacuum annealed at  $10^{-6}$  Torr and  $\sim 1000$  °C for 10 hr. The final metal content after this purification process, as determined by ash analysis (combustion in dry air) in a gravimetric apparatus, yielded a value of 0.2 at % metal. Typical high resolution transmission electron microscope (HRTEM) images showed that the nanotubes were present in long bundles, with a bundle diameter in the range 10–15 nm, i.e., containing  $\sim 100$ –200 tubes. The material was also found to exhibit the characteristic  $T=300$  K Raman spectrum (514 nm excitation) published previously, including the radial breathing mode band centered at  $186\text{ cm}^{-1}$  and the stronger tangential mode band at  $1593\text{ cm}^{-1}$ . The tube diameter distribution in this material is mainly confined to the range  $1.2 < d < 1.6$  nm, based on Raman spectra of the radial breathing modes collected at six different excitation wavelengths. TEP was measured *in situ* in a high vacuum apparatus using a heat pulse technique described previously.<sup>9</sup> The resistance was measured by a conventional four-probe method at 100 Hz. The sample temperature was varied over the range  $4\text{ K} < T < 500\text{ K}$ .

### III. RESULTS AND DISCUSSION

#### A. Effects of uniaxial stress on the TEP and resistance

It has been argued<sup>10,11</sup> that the measured TEP of a SWNT network may be affected by rope-rope contacts in the mat or film and their random orientation relative to the thermal gradient. This is a reasonable concern, particularly if we note that a SWNT network consists of ropes, themselves containing metallic and semiconducting tubes loosely touching each other through semiconducting tubes and/or amorphous carbon on the rope surface not eliminated by the purification process. In this picture, the TEP could be the result of a pathway of semiconducting tubes broken by series-connected intertube barriers, where the thermopower through the insulating barriers is described by either an activated, hopping-like conduction<sup>10</sup> or a fluctuation-induced tunneling model.<sup>11</sup> We investigated the possible influence of rope-rope contacts on the four-probe resistance [Fig. 1(a)] and the TEP

[Fig. 1(b)] of thin film or mat samples by observing the change in these quantities under the action of uniaxial stress. The experimental geometry is shown schematically in the inset to Fig. 1(b). The measurements were made in air at  $T \approx 300$  K as a function of the loading force  $F$  applied normal to the substrate supporting the SWNT rope film. Thermocouples [TC(1), TC(2)] and current leads [I(1), I(2)] made contact to the film via Ag epoxy outside the region of applied stress. When the four-probe resistance was being measured, current was passed via the leads [I(1), I(2)] and one arm of each TC was used for the voltage measurement. The pressure was calculated directly from the cross-sectional surface area of the insulating rod [inset, Fig. 1(b)].

As can be seen in Fig. 1, the applied force (stress) impacts  $R$  but not the TEP (or Seebeck coefficient  $S$ ). It should be noted that the data are for two oxygen-doped samples under ambient conditions. If the contacts regions between the ropes dominated the thermopower, once these regions become better heat conductors under applied stress, the thermopower would be expected to decrease. However, as shown in Fig. 1(b), the pressure has little effect on the thermopower. The insensitivity of  $S$  to the improved rope-rope contact resistance, observed via the decreasing  $R$  in Fig. 1(a), is taken as direct evidence that the contact barrier between ropes is not significantly involved in the TEP of the SWNT film.

#### B. Compensation doping and defect chemistry

We assume that each rope consists of a mixture of metallic and semiconducting tubes, in the approximate ratio of 1:2. There are probably defect states in the tubes, of which some are donors and some are acceptors. Prior calculations have shown that defects in metallic nanotubes introduce resonances in the density of states at the Fermi energy. They are discussed in a later section. Donors in a semiconducting tube introduce an additional electron into the system, while acceptors contribute an additional hole. In both cases, we show in the Appendix that the additional electron or hole is transferred to the metallic tubes, and controls the chemical potential of the rope. Specifically, we assign the acceptor states to chemisorbed oxygen. Calculations by Jhi *et al.*<sup>12</sup> predicted a charge transfer of about 0.1 electron to the  $\text{O}_2$  molecules in contact with the semiconducting tube wall. The origin of the donor state is less clear. It may be associated with the wall defects.

Figure 2 shows the time evolution of thermopower at  $T=500$  K for a typical purified thin film sample under vacuum. The sample was previously exposed to air under ambient conditions for several days, then mounted in the measuring apparatus and evacuated to  $10^{-6}$  Torr and heated from 300 to 500 K. At point A, the sample is still nearly air saturated which was accomplished under ambient conditions. The observed behavior at  $T=500$  K is in agreement with previously reported results on similar samples.<sup>6,13</sup> As the sample was degassed at  $T=500$  K in vacuum, the thermopower was observed to decrease slowly from an initial value  $S = +8\text{ }\mu\text{V/K}$ , changed sign at B (fully compensated state), and then gradually approached a constant value of  $S = -10\text{ }\mu\text{V/K}$  near C (fully degassed state). Exposure of the

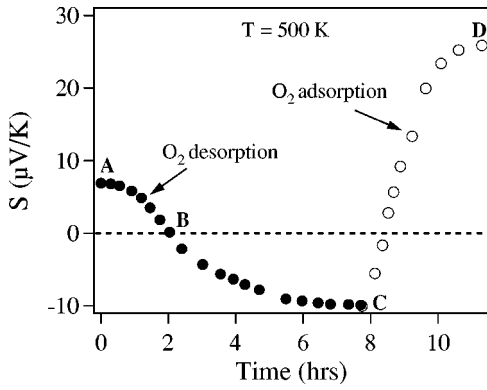


FIG. 2. Thermopower response to vacuum and O<sub>2</sub> (1 atm) at  $T=500$  K. (A→C): Vacuum degassing of a sample initially O<sub>2</sub> doped under ambient conditions for several days. (C→D): Exposure of the degassed sample to 1 atm of O<sub>2</sub> established at C. The TEP remains “locked” at the value  $S=+25\mu\text{V/K}$  at D, i.e., subsequent vacuum degassing has no effect on  $S$ .

fully degassed film to 1 atm of pure oxygen  $T=500$  K, *irreversibly* changed the thermopower to a large, positive value at  $S=+25\mu\text{V/K}$  as indicated by the point labeled D (high- $T$  O<sub>2</sub>-doped state) in Fig. 2. This indicates that O<sub>2</sub> exposure at  $T=500$  K results in a more strongly bound oxygen acceptor, possibly a C-O bond. When vacuum was applied at D, we were unable to change the TEP.

Figure 3 displays the temperature dependence of TEP for the same sample at the points A, B, C, and D indicated in Fig. 2. The series of curves  $S(T)$  also labeled A, B, and C in Fig. 3 are observed after successively longer periods of vacuum degassing which removes successively larger amounts of O<sub>2</sub> from the ropes. We note that it is possible to reliably tune to any intermediate *metallic* TEP between the air-saturated state and the fully degassed state, including an almost zero TEP state (curve B). For example, the TEP for the initially air-saturated sample (under ambient conditions) and the same sample oxygen doped by exposure at  $T=500$  K to 1 atm O<sub>2</sub>,

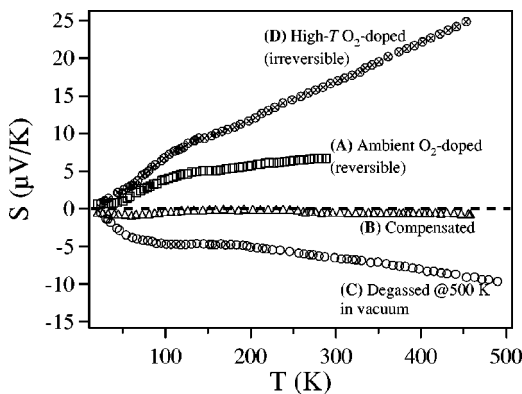


FIG. 3. Temperature dependence of the thermopower  $S$  for a SWNT thin film after successively longer periods of O<sub>2</sub> degassing at  $T=500$  K in vacuum. The labels A, B, and C refer to a vacuum degassing interval indicated in Fig. 2. Curve D is for the same sample exposed to 1 atm O<sub>2</sub> at  $T=500$  K for about 4 hr after being fully degassed to point C.

are both positive and almost linear over the entire temperature range. A positive “knee” is observed around 120 K, and changes sign tracking the sign of the linear background on which it is superimposed. The TEP for the degassed sample, on the other hand, is negative over the entire temperature range and also shows a linear metallic variation with temperature at high temperatures, with a superimposed negative “hump” around 80 K. A low- $T$  hump is often identified with phonon drag,<sup>14</sup> which enhances the diffusion thermopower. Our assignment of phonon drag is consistent with the sign change of the hump. Phonon drag is associated with the flux of phonons from the hot end to the cold end of the sample which “drags” additional carriers to the cold end, enhancing the thermopower.

### C. Model calculations of $S$ using tight binding bands

The TEP behavior of the SWNT film, as shown in Figs. 1–3, is consistent with a diffusion thermopower dominated by metallic tubes in a rope. The metallic character of the TEP can be understood from the following argument. The thermopower for a rope can be written as the sum of the conductance-weighted contributions from all tubes in a rope because they are connected in parallel,

$$S = \frac{1}{\sigma} \sum_{j=1}^N \sigma_j S_j, \quad (1)$$

$$\sigma = \sum_{j=1}^N \sigma_j, \quad (2)$$

where the index  $j$  runs over all  $N$  tubes in a rope,  $\sigma_j$  and  $S_j$  are the conductance and the thermopower of the  $j$ th tube, and  $\sigma$  is the conductance of the entire rope. If the semiconducting tubes are not degenerately doped,  $\sigma_j(\text{metal}) \gg \sigma_j(\text{semiconductor})$  and we find  $S \sim \langle S_j(\text{metal}) \rangle$  and  $\sigma \sim N/3 \langle \sigma_j(\text{metal}) \rangle$ , where  $\langle \rangle$  indicates the average value, and the result for  $\sigma$  assumes a statistical average number of metallic tubes in a rope. If some semiconducting tubes are degenerately doped, they would mimic to some extent the temperature dependence of the conductivity and the thermopower of the metallic tubes. Specifically, the TEP for the degenerately doped semiconducting tubes would exhibit a  $S \sim T/E_F$  behavior, but  $E_F$  is small, so TEP for these tubes would be high. The relative contribution of the degenerately doped semiconducting tubes would be controlled by their  $\sigma_j$  [Eq. (2)], and we anticipate that this conductance is significantly lower than for intrinsic metallic tubes. There is no clear evidence that some of the tubes in our samples are degenerately doped semiconducting tubes, but if they exist they may enhance a metallic thermopower.

We note that the thermopower has been shown (Fig. 1) to not depend on the rope-rope contacts, but the film resistance is affected. The value of  $\sigma$  one might compute from Eq. (2) does not represent the mat/film conductance, i.e., the rope-rope contact resistance is in series and must be added into the calculation.

We next show that the magnitude of the experimental TEP cannot be explained by a simple two-band model for a me-

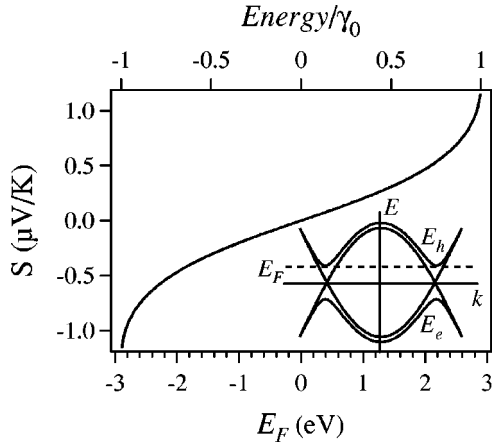


FIG. 4. Calculated thermopower of an (10,10) carbon nanotube as a function of the Fermi level position.

talic tube with electron-hole symmetry, except for the fully compensated sample. To show this, we take the simplifying assumption that our samples are mainly composed of metallic (10,10) tubes, whose band structure near  $E_F$  is characterized by two pairs of one-dimensional tight binding bands. These pairs are shown in the inset to Fig. 4, together with the next highest- (lowest-)lying bands. In the frequently used two-band model for the TEP, one obtains

$$S = (\Sigma_1/\Sigma)s_1 + (\Sigma_2/\Sigma)s_2, \quad (3)$$

where  $\Sigma_j$  and  $s_j$  are, respectively, the conductivity and the thermopower of the  $j=1,2$  band, and  $\Sigma = \Sigma_1 + \Sigma_2$  is the total conductivity. The diffusion thermopower for a given band can be calculated via the Boltzman transport equation using the standard Mott formula<sup>14</sup> for metallic conduction

$$S_d = -\frac{\pi^2 k_B^2 T}{3|e|} \left\{ \frac{d \ln \sigma(E)}{dE} \right\}_\mu, \quad (4)$$

where  $k_B$  is the Boltzman constant,  $T$  is the temperature,  $e$  is the electronic charge,  $\sigma(E)$  is the band conductivity per unit energy  $E$ , and  $\mu = E_F$  is the Fermi energy. The conductivity  $\sigma(E)$  is given by the well known relation

$$\sigma(E) = e^2 v(E)^2 D(E) \tau(E). \quad (5)$$

Here  $v$  is the free carrier velocity,  $D(E)$  the density of states, and  $\tau$  the carrier relaxation time. Equations. (4) and (5) are used in Eq. (3) together with a power law form  $\tau(E) \sim E^m$ . To compute  $v$  and  $D(E)$  we have used the tight binding bands given by

$$E_e = \gamma_0 \left[ 1 - 2 \cos\left(\frac{ka_0}{2}\right) \right], \quad (6a)$$

$$E_h = -\gamma_0 \left[ 1 - 2 \cos\left(\frac{ka_0}{2}\right) \right], \quad (6b)$$

where  $e, h$  refer to the electron and hole bands crossing at  $E_F$ ,  $a_0 = 1.42 \times \sqrt{3} \text{ \AA}$  is the lattice constant for a 2D

graphene sheet, and  $\gamma_0 = 2.9 \text{ eV}$  is chosen for the nearest-neighbor C-C overlap integral.

In Fig. 4, we plot the result for  $S$  at  $T = 300 \text{ K}$ , for  $\tau_{e,h} \sim E^{3/2}$  as a function of  $\mu = E_F$ . We allow the Fermi energy to move up or down in rigid  $\pi$  bands in response to the balance between donor and acceptor impurities. We note that moving  $E_F$  by as much as  $\pm 1 \text{ eV}$  relative to the mirror symmetry plane in the band structure generates only  $\sim 0.25 \text{ } \mu\text{V/K}$  for  $S$  at  $T = 300 \text{ K}$ , which is a factor of 40 less than the experimental data for  $\text{O}_2$ -doped material or fully degassed material. On the other hand, the TEP of a fully compensated sample ( $S \sim 0$ ) is consistent with this calculation (curve  $B$ , Fig. 2), in agreement with early theoretical calculations.<sup>3</sup>

Therefore, although the TEP of a compensated sample can be understood on the basis of our model and using mirror symmetry bands [Eq. (6)], the same calculation appears to be unable to explain the large positive or negative values of  $S$  in the doped material.

#### D. Thermopower from enhanced $D(E_F)$ due to impurities

Previous calculations of TEP in a doped metallic tube provide an explanation for these large values of TEP.<sup>15,16</sup> These calculations report that the density of states of metallic SWNT's containing nitrogen impurity donor states exhibit a broad resonance in the density of states near the chemical potential. These broad resonances have been identified as the donor bound states derived from the next highest-lying electron band. Electron states in the metallic bands that cross near  $E_F$  overlap in energy with these bound states and create a broad resonance state. The conduction electrons in the metallic bands can spend part of their time in a virtual bound state of the donor. The broad resonances in the density of states  $D(E)$  overlap the chemical potential, and provide a larger nonzero value for  $S$ , consistent with an enhanced  $D(E)$ . An additional contribution to the TEP may be provided by the carrier lifetime  $\tau(E)$ . This quantity has not yet been calculated.

According to Ref. 16, boron is an acceptor impurity, and its broad  $D(E)$  resonances are from holes bound to the next lowest-lying holelike band in the metallic tubes. Here the resonance is below the chemical potential, and the TEP will have the opposite sign compared to the case where donor impurities are dominant. We suspect that these metallic DOS resonances located near  $E_F$  can occur for many different impurities.

#### E. Phonon drag

We now discuss the low- $T$  contribution to  $S$  from phonon drag. In the free electron approximation, when the phonons are assumed to have a Debye spectrum, and in the absence of Umklapp scattering, the phonon-drag thermopower  $S_g$  for metals is given by

$$S_g = \frac{c_v}{N_e} \alpha, \quad (7)$$

where  $c_v$  is the lattice specific heat per atom,  $N$  is the number of conduction electron per atom, and  $\alpha$  is a ‘‘transfer factor,’’ which lies between 0 and about 1.  $\alpha$  is a measure of the relative probability of a phonon-electron collision.

At low temperatures,  $c_v \sim T^n$ , where  $n > 1$ . The precise exponent  $n$  depends on the detailed phonon dispersion relations and the dimensionality of the system. For 3D graphite,  $c_v$  presents a superlinear behavior below 100 K. A nanotube bulk sample presents 3D behavior similar to that of graphite only when tubes in the bundles are strongly coupled.<sup>17</sup> For tubes weakly coupled in a rope, or individual tubes  $c_v \propto T$ . On the other hand, phonon-drag thermopower decays as  $1/T$  at higher temperatures, because phonon-phonon collisions increase linearly with temperature.

The shape of the temperature dependence of the TEP for a degassed sample (curve C, Fig. 3) suggests that phonon drag may be responsible for the *negative* peak observed at  $\sim 100$  K. As in typical metals, the phonon-drag contribution should become negligible around room temperature. We also find that the strength of this peak is suppressed by oxygenation of the sample (Fig. 3). With increasing concentration of oxygen in the film, the phonons should be more strongly scattered by the  $O_2$  impurity centers ( $O_2^-$ , C–O bonds) and are therefore expected to transfer less momentum to the conduction electrons. The phonon drag enhancement would be expected to be reduced in this case.

If the observed peak at  $\sim 100$  K in the TEP is indeed due to phonon-drag effects, systematic TEP measurements at low temperatures down to at least 1 K should reveal a considerable amount of information on phonon scattering and interaction with conduction electrons and defects in the tubes. It is expected that phonon drag should be particularly strong in one-dimensional systems. A calculation of this effect is in progress.<sup>18</sup>

#### ACKNOWLEDGMENTS

This work was supported by funds from ONR Grant No. DAAB07-97-C-J036.

#### APPENDIX

Let  $N$  be the density of donors in a single semiconducting tube. The donors can be either neutral ( $N^x$ ) or else ionized ( $N^*$ ), so  $N = N^x + N^*$ . Assuming two semiconducting tubes per metallic tube, charge neutrality states that the negative charges, from the metallic tube ( $n_{me}$ ) and the two semiconducting tubes ( $n_{se}$ ), equals the density of positive charges from the ionized donors and holes ( $n_{sh}$ )

$$n_{me} + 2n_{se} = 2N^* + 2n_{sh}. \quad (A1)$$

These various quantities must be related to a single variable. First, we use the definition of  $n_{se}$ ,

$$n_{se} = 2 \int \frac{dk}{2\pi} e^{\beta[\mu - \varepsilon_S(k)]}, \quad (A2a)$$

$$n_{se} \approx n_0 e^{-\beta(E_G/2 - \mu)}, \quad (A2b)$$

$$n_0 = \frac{4\sqrt{k_B T}}{3a_{C-C}\sqrt{\pi\lambda E_G}} \approx \frac{1}{8.5 \text{ nm}}, \quad (A2c)$$

$$\lambda = \frac{-2 \cos(q\pi/N)}{|1 + 2 \cos(q\pi/N)|^2} \approx 90.0. \quad (A2d)$$

In Eqs. (A2),  $\mu$  is the chemical potential,  $\varepsilon_S(k)$  is the conduction band edge of the semiconducting tubes,  $E_G$  is the semiconducting gap, and  $N=11$ . We have used the tight binding band for a (11,0) zigzag tube as a typical example. The values for  $n_0$  and  $\lambda$  were obtained using these values.

The variable to solve in Eq. (A1) is  $x = n_{se}/n_0$ . The hole density is found from the  $n-p$  product

$$n_{se}n_{sh} = n_0^2 e^{-\beta E_G} \equiv (\alpha n_0)^2, \quad (A3a)$$

$$\alpha = e^{-\beta E_G/2}, \quad (A3b)$$

where  $1/\beta = k_B T$ .

The chemical equilibrium between ionized and neutral donors is given by the rate equation

$$n_{se} = 2n_0 \frac{N^x}{N^*} \gamma, \quad \gamma = e^{-\beta E_D}, \quad (A4)$$

where  $E_D$  is the donor binding energy with respect to the conduction band minimum. Solving the above equation gives

$$N^* = 2N_D \frac{\gamma}{x + 2\gamma}. \quad (A5)$$

Next consider the metallic tube. We assume it is charge neutral if the chemical potential is at the energy  $\varepsilon_m = 0$  where the bands cross. If this point is defined as  $\mu = 0$ , then the excess charge density on the metallic tube is

$$n_{me} = \rho_m \mu = k_B T \rho_m \ln\left(\frac{x}{\alpha}\right), \quad (A6a)$$

$$\rho_m = \frac{8}{3\pi a_{C-C} \gamma_0}, \quad (A6b)$$

where  $\mu$  is evaluated using Eq. (A2b) and  $\rho_m$  is the total density of states for the four metallic bands.

Using these variables, the charge [Eq. A1] can be written as

$$0 = x - \frac{\alpha^2}{x} + s \ln(x/\alpha) - r \frac{2\gamma}{x + 2\gamma}, \quad (A7a)$$

$$s = \frac{k_B T \rho_m}{2n_0}, \quad r = \frac{N}{n_0}. \quad (A7b)$$

At  $r=0$  (i.e., no donors), the solution is  $x = \alpha$ . In this case, the chemical potential is at midgap, and there are equal numbers of electrons and holes in the semiconductor. There is no charge transfer to the metallic tubes. In this case  $x \sim O(10^{-5})$ .

In the limit of low doping, then  $r$  is small. We assume that  $\alpha \ll \gamma$ , or that the donor bonding energy is less than  $E_G/2$ . In that case, the last two terms in the basic equation (A7a) are the largest and must cancel

$$x = \alpha \exp(r/s). \quad (\text{A8})$$

In this situation, there is complete charge transfer. All of the donors ionize and transfer their electrons to the metallic tube. Thus, there is negligible electrical conductivity in the nonde-

generate semiconducting tubes. The chemical potential rises in the metallic tube, but by a small amount. In equilibrium, the chemical potential must be the same for all tubes. If the donor density becomes large, then the chemical potential approaches the donor energy in the semiconductor. Then the charge transfer lessens for additional donors. Because of the charge transfer, there is negligible electrical conductivity in the semiconducting tubes. A similar analysis applies if the defects are acceptors.

---

\*Author to whom correspondence should be addressed. Email address: pce3@psu.edu

- <sup>1</sup>M.S. Dresselhaus, G. Dresselhaus, and P.C. Eklund, *Science of Fullerenes and Carbon Nanotubes* (Academic, San Diego, 1996); S. Saito, G. Dresselhaus, and M.S. Dresselhaus, *Physical Properties of Carbon Nanotubes* (Imperial College Press, London, 1998); *The Science and Technology of Carbon Nanotubes* edited by K. Tanaka, T. Yamabe, and K. Fukui (Elsevier, New York, 1999).
- <sup>2</sup>L. Grigorian, K.A. Williams, S. Fang, G.U. Sumanasekera, A.L. Loper, E.C. Dickey, S.J. Pennycook, and P.C. Eklund, *Phys. Rev. Lett.* **80**, 5560 (1998).
- <sup>3</sup>J. Hone, I. Ellwood, M. Muno, A. Mizel, M.L. Cohen, A. Zettl, A.G. Rinzler, and R.E. Smalley, *Phys. Rev. Lett.* **80**, 1042 (1998).
- <sup>4</sup>L. Grigorian, G.U. Sumanasekera, A.L. Loper, S.L. Fang, J.L. Allen, and P.C. Eklund, *Phys. Rev. B* **60**, R11 309 (1999).
- <sup>5</sup>T.W. Odom, J.-L. Huang, C.L. Cheung, and C.M. Lieber, *Science* **290**, 1549 (2000).
- <sup>6</sup>G.U. Sumanasekera, C.K.W. Adu, S. Fang, and P.C. Eklund, *Phys. Rev. Lett.* **85**, 1096 (2000).
- <sup>7</sup>P.G. Collins, K. Bradley, M. Ishigami, and A. Zettl, *Science* **287**,

- 1801 (2000).
- <sup>8</sup>V. Derycke, R. Martel, J. Appenzeller, and P. Avouris, *Nano Lett.* **1**, 453 (2001).
- <sup>9</sup>G.U. Sumanasekera, L. Grigorian, and P.C. Eklund, *Meas. Sci. Technol.* **11**, 273 (2000).
- <sup>10</sup>M. Baxendale, K.G. Lim, and G.A.J. Amaratunga, *Phys. Rev. B* **61**, 12 705 (2000).
- <sup>11</sup>G.C. McIntosh and A.B. Kaiser, *Curr. Appl. Phys.* **1**, 145 (2001).
- <sup>12</sup>S.-H. Jhi, S.G. Louie, and M.L. Cohen, *Phys. Rev. Lett.* **85**, 1710 (2000).
- <sup>13</sup>K. Bradley, S.-H. Jhi, P.G. Collins, J. Hone, M.L. Cohen, S.G. Louie, and A. Zettl, *Phys. Rev. Lett.* **85**, 4361 (2000).
- <sup>14</sup>R.D. Barnard, *Thermoelectricity in Metals and Alloys* (Wiley, New York, 1972).
- <sup>15</sup>T. Kostyrko, M. Bartkowiak, and G.D. Mahan, *Phys. Rev. B* **59**, 3241 (1999); **60**, 10 735 (1999).
- <sup>16</sup>P.E. Lammert, V.H. Crespi, and A. Rubio, *Phys. Rev. Lett.* **87**, 136402 (2001).
- <sup>17</sup>J. Hone, B. Batlogg, Z. Bense, A.T. Johnson, and J.E. Fischer, *Science* **289**, 1730 (2000).
- <sup>18</sup>V.W. Scarola, G.D. Mahan, and J.K. Jain (unpublished).